Supporting information

Van der Waals interactions in the self-assembly of 5-amino [6]helicene on Cu(100) and Au(111)

S1. STM experiments and chemicals

The experiments were carried out in an ultrahigh vacuum system equipped with a variable-temperature STM from Omicron Nanotechnology. The base pressure of the chamber was in the low 10^{-10} mBar range.
The Cu(100) and Au(111) surfaces were prepared by cycles of sputtering with Ar at 1.5 keV and annealing at 770 K.
The M-**AH** molecules were evaporated from a resistivity heated BN crucible at a rate of about 0.2 monolayer (ML) per minute. The molecules were dosed on the Cu(100) and Au(111) surfaces at RT. During the evaporations the pressure was in the low 10^{-9} mBar range.
After the preparation, the samples were transferred to the STM sample holder which was already cooled at 100K. The STM images were obtained at 100 K using W tips. Negative sample bias voltages correspond to occupied-state images. The thermal drift was compensated automatically in real time.
The coverages informed are calculated as a percentage of the ideal saturation coverage, taking into account the density of the unit cells in the high coverage phases. For the unit cell of tetramers on Cu(100) we have δ=7.1x 10^{-3} molecules/Å^2 and for the dimer-row phase on Au(111) δ=8.3x 10^{-3} molecules/Å^2.

5-Amino[6]helicene
1H NMR (DMSO-d_6) δ8.12 (d, 1H), 7.93-8.05 (m, 3H), 7.89 (d, 1H), 7.82 (d, 1H), 7.49 (d, 1H), 7.46 (dd, 1H), 7.21 (t, 2H), 7.07 (s, 1H), 6.61-6.69 (dq, 2H), 6.13 (bs, 2H)

13C NMR (DMSO-d_6) δ144.8, 136.7, 134.1, 131.9, 131.6, 131.2, 130.1, 128.3, 128.1, 127.7, 127.1, 126.8, 126.0, 125.7, 125.4, 125.1, 124.5, 124.3, 122.7, 120.6, 104.0, 98.1, 91.6

[M+1](API/ES) calculated: 344.14 found: 344.1 CD data for 5-Amino-hexahelicene with an e.e. of 99% and a chemical purity of 93%

$\Delta\varepsilon = \Theta / (32980 * c * l) = 55.1/(32980x0.000013x1) = 128.5$ mdeg/mol/l/cm at 248 nm and 35.0/(32980x0.000013x1) = -81.6 mdeg/mol/l/cm at 334 nm with a concentration of 0.013 mmol/L in MeOH
The compound is stable in solid state, but oxidizes in solution on exposure to air to give strongly colored material(s), likely due to oxidation of the amino group. This makes the purity determinations by HPLC difficult to interpret, since traces of strongly colored materials can give rise to large peaks in the HPLC using UV detection.
This was tested by measuring one HPLC sample immediately after chromatography. HPLC analysis indicated a purity of 95%. When the sample was left overnight and measured again, the purity of the same sample as determined by HPLC had deteriorated to 90%, although no impurities could be seen in the 1H NMR spectra.

The material used had a purity >95% for the (-)-enantiomer and >90% for the (+)-enantiomer according to NMR analysis, and an e.e. >99% for the (-)-enantiomer and >96% for the (+)-enantiomer
The details for two batches, *based* on HPLC data and NMR spectra, are given.
The analytical data may be summarized as follows:

Peak 1 ((M)-(-)-enantiomer):
>98% pure according to HPLC
>95% pure according to NMR
>99% e.e. according to chiral HPLC

After several experiments under UHV, the color of the remaining powder was checked visually for stability. The persistent ocre color is an indication of the absence of oxidation products.

S2. Computational Methods

The DFT calculations were performed using the Quantum ESPRESSO package [1], which is an implementation of the plane-wave with ultrasoft-pseudopotentials approach. In order to treat adequately the vdW interactions, the correlation part of the energy was treated using the second version of van der Waals density functional (vdW-DF2) [2-5].
For the surface calculations we used the slab method, with four Cu layers. For all the calculations, we fixed the two lower layers while all other atoms were allowed to relax. We used a wave-function/charge cutoff of 30/300 Ry, and Brillouin integrations were done using a grid equivalent to 12x12x1 and 16x16x1 k-points for the surface unit cell of Cu(100) and Au(111), respectively.
For the adsorption of **AH** on Cu(100) we used a $3\sqrt{2}$ x3 $\sqrt{2}$ R45° supercell with lattice vectors **a** = **b** = 11.22Å. For the adsorption of **AH** Au(111) we used a 4 x4 supercell with lattice vectors **a** = **b** = 12.36 Å. To model and estimate the molecule-molecule interaction in the ordered phase, we performed calculations with the experimental unit cell and the observed number of molecules but without the substrate. In order to simulate the effect of the substrate, the molecules are allowed to relax but keeping the *z* position of the lower C-rings fixed at the relaxed configuration when adsorbed.
The STM images are simulated using the Tersoff-Hamann aproximation in which the current is proportional to the integrated local density of states (ILOS), in a range given by the applied bias. For a constant current simulation one needs an isodensity surface of this ILOS. The simulated images correspond to unsupported models where the substrate is absent. As a consequence, the ILOS in the region between the groups of molecules is too low, therefore it is not posible to produce an isodensity surface. We have therefore simulated the STM images in the constant height mode. Nevertheless, as our simulation is not used to compare critical submolecular features but just geometrical distances in the calculated unit cell in comparison with the experimental values, constant height simulations are useful to this purpose.

2.1 AH/Cu(100)

We considered both the molecule with the amine group close to the surface ("N-down" configuration) and the molecule with the amine group far from the surface ("N-up" configuration).
The N-down configuration has the higher adsorption energy by 0.085 eV.

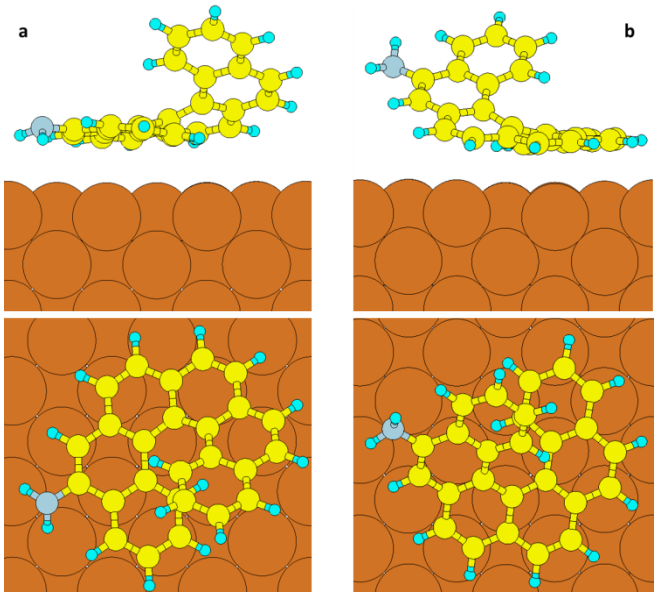

1.57 eV 1.49 eV

*Figure **S1**: DFT relaxed configurations and adsorption energies for M-**AH** on Cu(100): (a) N –down configuration (side and top view); and (b) N-up configuration (side and top view)*

In Fig. **S2** we show the density of states (DOS) for the **AH** molecule in gas phase, and the proyected DOS on the molecules when adsorbed on the Cu(100) surface. Both DOS are very similar, indicating that there is no covalent bond formation. Moreover, when the molecule is adsorbed the Fermi level lies close to the midpoint of the organic HOMO-LUMO gap, a sign that there is no charge transfer between molecule and surface.

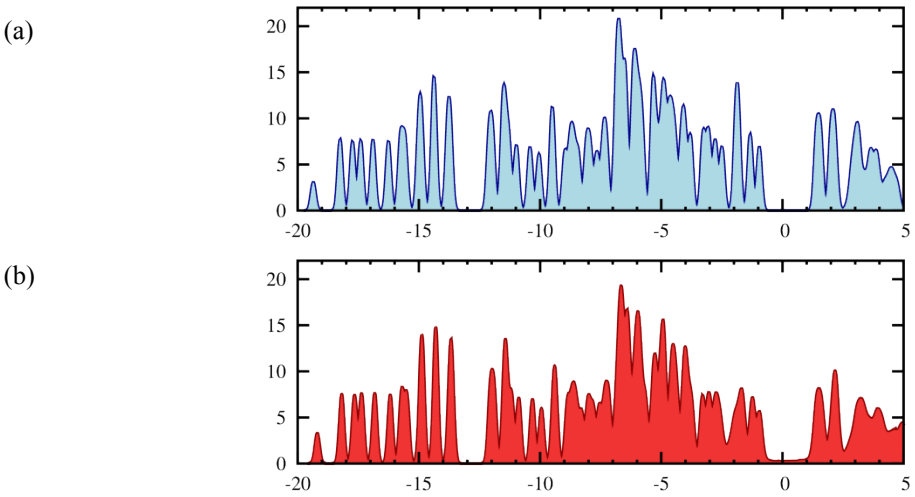

Figure **S2**: (a*) Density of states of **AH** in gas phase. (b) Projected density of states on **AH** when adsorbed on Cu(100).*

2.2 Unsupported structures on Cu(100)

We considered several configurations for the assembly of M-**AH** on Cu(100) compatible with the experimental STM images. Fig. S**3** shows two structures, for the higher adsorption energy (N-down) configuration with the amine groups pointing out of and into the tetramer. The lowest energy correspond to the amine groups pointing outward with an interaction energy of -0.51 eV (-0.127 eV/molecule). In Fig. **S4** we show the simulated image for this configuration. While weak vdW interactions determine the assembly of the tetramers, once formed the tetramer structures are mutually repulsive. Therefore, a closer packing is not observed.

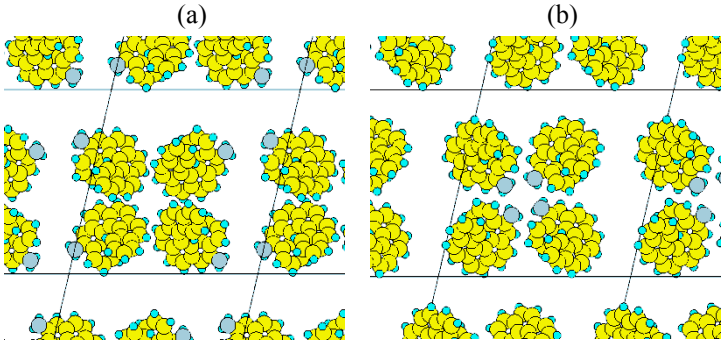

-0.51 eV -0.05 eV

*Figure **S3**: DFT relaxed configurations and interaction energies per unit cell for M-**AH** on Cu(100): (a) with amine groups pointing out of the tetramer; and (b) with amine groups pointing into the tetramer.*

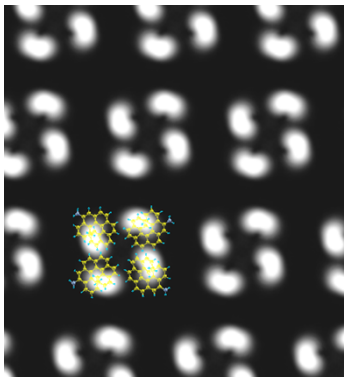

*Figure **S4**: Simulated STM image of M-**AH** on Cu(100), forming a tetramer with N-down molecules.*

As we also observed duplets, tripletss, and rows for lower coverage of **AH** on Cu(100), we considered the formation of these structures in gas phase models. For isolated dimers and trimers we obtained interaction energies of -0.21 eV (-0.103 eV/molecule) and -0.32 eV (-0.106 eV/molecule). For rows of dimers (as seen in Fig. 1 b in the main text) the interaction energy is -0.24 eV (-0.121 eV/molecule). Fig. **S5** shows some possible conformers for this dimers, trimers and rows with the corresponding energies. We notice that all the structures have similar energies and therefore is not surprising to observe the occurrence of all of them, being the tetramers (Fig **S3** (a), -0.121eV/ molecule) favored at high coverage .

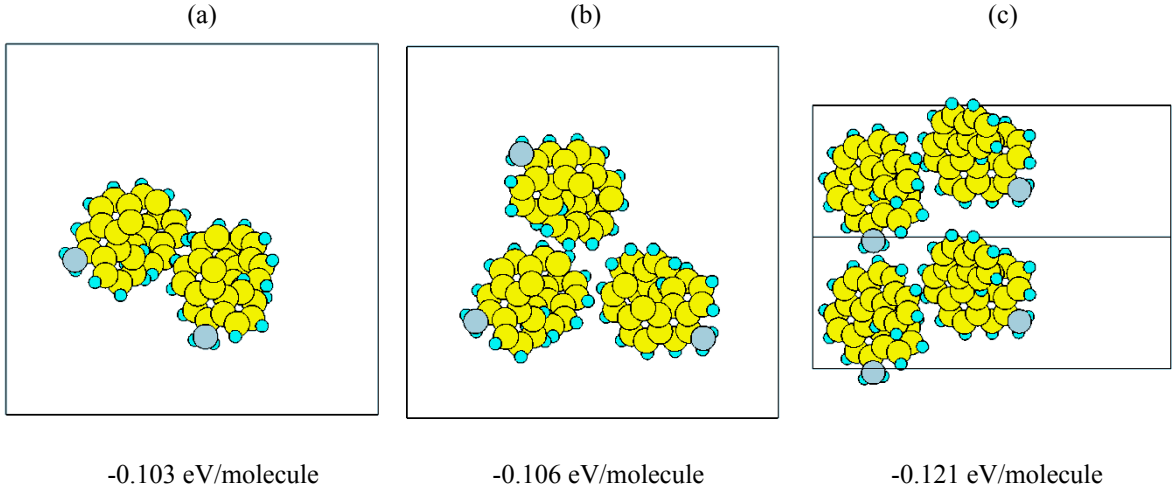

*Figure **S5:** DFT relaxed configurations and interaction energies per unit cell for order configurations of M-**AH** on Cu(100): (a)dimers; (b)trimers; (c) rows of dimers.*

2.3 Amino-helicene/Au(111)

We considered both the molecule with the amine group close to the surface (“N-down" configuration) and the molecule with the amine group far from the surface (“N-up" configuration). The N-down configuration has the higher adsorption energy by 0.26 eV.

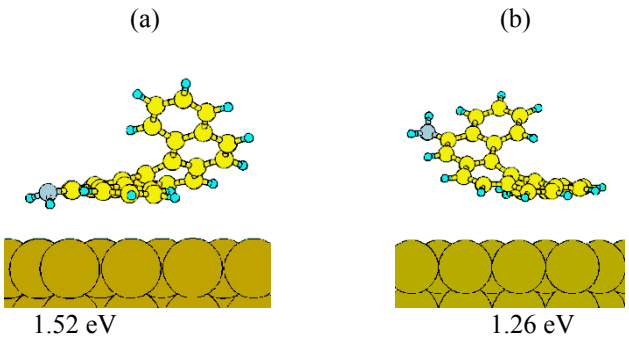

*Figure **S6**: DFT relaxed configurations and adsorption energies for M-**AH** on Au(111): (a) N –down configuration (side view); and (b) N-up configuration (side view)*

2.4 Unsupported strutures on Au(111)

We considered several configurations for the assembly of **AH** on Au(111) compatible with the experimental STM images. We notice that the closest distance between the molecules forming the double rows on Au(111) (6.7 ±0.5) Å is reduced in comparison to the rows assembled on Cu(100), Fig. 1b, (10.0 ±0.5) Å. The same trend is observed for the p_3 and p_4 structures embedded in the disordered region. We attribute this to the lower interaction of the C6 rings to the Au surface that allows the molecules to get closer to maximize the vdW interactions. Fig. **S7** shows the lower energy configuration of the double rows with interaction energy of -0.14 eV per unit cell.

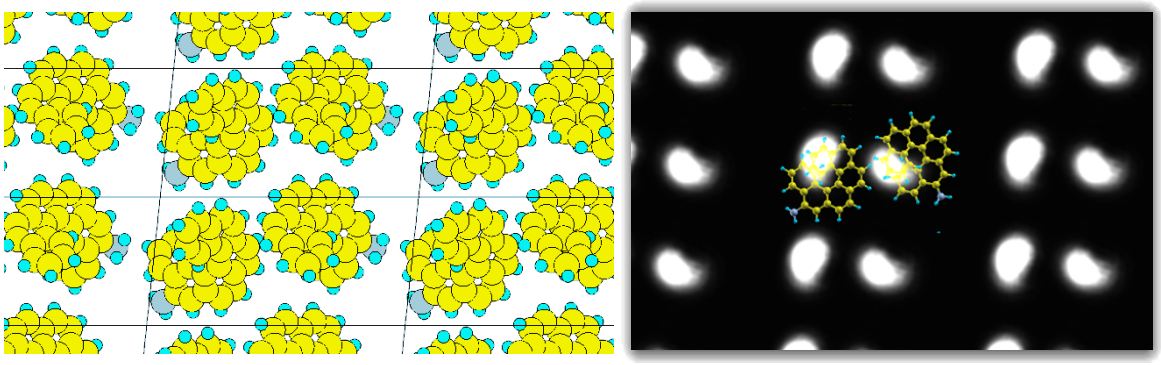

(a) (b)

*Figure **S7**: (a) DFT relaxed configurations for the lowest energy configuration of **AH** on Au(111).(b) corresponding STM simulated image.*

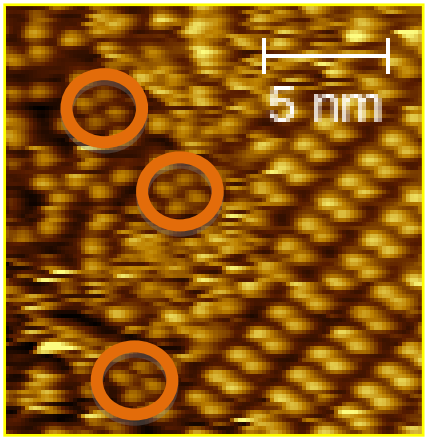

*Figure **S8**: STM image highlighting the quadruplet structures embedded in the disordered region for M-**AH** on Au(111): closest intermolecular distance : Rows:* (6.7 ±0.5) Å*: Quadruplets:* (7.3 ±0.5) Å

References

[1] P. Giannozzi, S. Baroni, N. Bonini, M. Calandra, R. Car, C. Cavazzoni, D. Ceresoli, G. L. Chiarotti, M. Cococcioni, I. Dabo, and et.al. J. Phys.: Condens. Matter, 21:395502, 2009.
[2] M. Dion, H. Rydberg, E. Schroder, D. C. Langreth, and B. I. Lundqvist. Phys. Rev. Lett., 92:246401, 2004.
[3] T. Thonhauser, V. R. Cooper, A. Puzder S. Li, P. Hyldgaard, and D. C. Langreth. Phys. Rev. B, 76:125112, 2007.
[4] G. Roman-Perez and J. M. Soler. Phys. Rev. Lett., 103:096102, 2009.
[5] K. Lee, _E. D. Murray, L. Kong, B. I. Lundqvist, , and D. C. Langreth. Phys. Rev. B, 82:081101, 2010.